Resident memory T cells in the atherosclerotic lesion associate with reduced macrophage content and increased lesion stability

Jong, M.J.M. de; Depuydt, M.A.C.; Schaftenaar, F.H.; Liu, K.; Maters, D.; Wezel, A.; ... ; Slütter, B.A.

Arteriosclerosis, Thrombosis, and Vascular Biology

ORIGINAL RESEARCH

Resident Memory T Cells in the Atherosclerotic Lesion Associate With Reduced Macrophage Content and Increased Lesion Stability

M.J.M. de Jong, M.A.C. Depuydt, F.H. Schaftenaar, K. Liu, D. Maters, Anouk Wezel, Harm J. Smeets, J. Kuiper, I. Bot, K. van Gisbergen, B. Slütter

BACKGROUND: Tissue resident memory T (T_{RM}) cells are a T-cell subset that resides at the site of prior antigen recognition to protect the body against reoccurring encounters. Besides their protective function, T_{RM} cells have also been implicated in inflammatory disorders. T_{RM} cells are characterized by the expression of CD69 and transcription factors Hobit (homolog of Blimp-1 [B lymphocyte–induced maturation protein 1] in T cells) and Blimp-1. As the majority of T cells in the arterial intima expresses CD69, T_{RM} cells may contribute to the pathogenesis of atherosclerosis as well. Here, we aimed to assess the presence and potential role of T_{RM} cells in atherosclerosis.

METHODS: To identify T_{RM} cells in human atherosclerotic lesions, a single-cell RNA-sequencing data set was interrogated, and T-cell phenotypes were compared with that of integrated predefined T_{RM} cells. The presence and phenotype of T_{RM} in atherosclerotic lesions was corroborated using a mouse model that enabled tracking of Hobit-expressing T_{RM} cells. To explore the function of T_{RM} cells during atherogenesis, RAG1$^{-/-}$ (RAG1 deficient) LDLr$^{-/-}$ (low-density lipoprotein receptor knockout) mice received a bone marrow transplant from Hobit$^{KO/CRE}$Blimp-1$^{flox/flox}$ mice, which exhibit abrogated T_{RM} cell formation, whereafter the mice were fed a Western-type diet for 10 weeks.

RESULTS: Human atherosclerotic lesions contained T cells that exhibited a T_{RM} cell–associated gene signature. Moreover, a fraction of these T cells clustered together with predefined T_{RM} cells upon integration. The presence of Hobit-expressing T_{RM} cells in the atherosclerotic lesion was confirmed in mice. These lesion-derived T_{RM} cells were characterized by the expression of CD69 and CD49α. Moreover, we demonstrated that this small T-cell subset significantly affects lesion composition, by reducing the amount of intralesional macrophages and increasing collagen content.

CONCLUSIONS: T_{RM} cells, characterized by the expression of CD69 and CD49α, constitute a minor population in atherosclerotic lesions and are associated with increased lesion stability in a Hobit and Blimp-1 knockout mouse model.

Key Words: allergy and immunology ■ atherosclerosis ■ memory T cells ■ T-lymphocytes ■ transcription factors

Atherosclerosis is a lipid-driven chronic inflammatory disease of the larger arteries resulting in vascular occlusion with clinical complications, including stroke and myocardial infarction. Various immune cell types inside the atherosclerotic lesions have been extensively studied, including T cells. Recent single-cell sequencing and cytometry techniques have identified T cells as one of the main immune cell populations in human and mouse atherosclerotic lesions.[1–4] Both CD4$^+$ and CD8$^+$ T cells are highly represented and exhibit a heterogeneous phenotype within the atherosclerotic lesion, encompassing distinct T-cell subsets and memory phenotypes.[1,2,5]

Interestingly, plaque resident T cells demonstrate significantly elevated CD69 expression compared with

Correspondence to: B. Slütter, PhD, Division of Biotherapeutics, Leiden University, Leiden Academic Centre for Drug Research, Einsteinweg 55, 2333 CC Leiden, the Netherlands. Email b.a.slutter@lacdr.leidenuniv.nl

Supplemental Material is available at https://www.ahajournals.org/doi/suppl/10.1161/ATVBAHA.123.320511.
For Sources of Funding and Disclosures, see page XXX.

Arterioscler Thromb Vasc Biol is available at www.ahajournals.org/journal/atvb

Nonstandard Abbreviations and Acronyms

Blimp-1	B lymphocyte–induced maturation protein 1
IL	interleukin
NK	natural killer
NKT	natural killer T
HLA	human leukocyte antigen
Hobit	Homolog of Blimp-1 in T cells
ITGA1	integrin alpha 1
ITGAE	integrin alpha E
LDLr$^{-/-}$	low-density lipoprotein receptor knockout
RAG1$^{-/-}$	RAG1 deficient
S1PR1	sphingosine-1-phosphate receptor 1
scRNA-seq	single-cell RNA sequencing
TGF-β	transforming growth factor beta
T_{RM}	resident memory T
ZNF683	zinc finger protein 683

Highlights

- A small fraction of resident memory T cells is detected in human atherosclerotic lesions.
- In murine atherosclerotic lesions, T_{RM} cells express CD69$^+$CD49α$^+$.
- Deletion of resident memory T cells is associated with reduced amount of intralesional macrophages and increased collagen content.

circulating T cells, with ≈60% of all T cells in the plaque expressing this molecule.[6] CD69 is a transmembrane C-type lectin and is upregulated upon TCR stimulation but can also be induced by other external stimuli such as exposure to type I IFN.[7] CD69 is involved in a variety of cellular processes, including proliferation and signal transduction, and controls tissue retention by regulating S1PR1 (sphingosine-1-phosphate receptor 1) expression.[8] Based on its function, CD69 can either be used as a marker for early TCR activation or for tissue residency in T cells.

Tissue resident memory T (T_{RM}) cells reside at the site of previous antigen encounter without access to the circulation and are primed to provide rapid and localized immune responses upon interacting with familiar antigens. Although T_{RM} cells are efficient in countering secondary infections, they have also been implicated in the involvement of chronic inflammatory diseases. T_{RM} cells are often enriched at sites of chronic inflammation.[9,10] Moreover, multiple studies have demonstrated the involvement of T_{RM} cells in reoccurring disease flares.[10,11] For example, in rheumatoid arthritis, disease reoccurrence was ameliorated by depleting T_{RM} cells.[11]

Yet, the involvement of T_{RM} cells in atherosclerosis remains elusive. T cells exhibiting a T_{RM} cell–like phenotype have been identified in human and mouse atherosclerotic lesions, and CD69$^+$ CD103$^+$ CD8$^+$ T cells with a T_{RM} cell–like phenotype were specifically expressed in human atherosclerotic lesions but not in blood.[2,12] Moreover, the majority of T cells in the atherosclerotic lesion has an effector memory phenotype, combined with high expression of CD69 (CCR7^{low}CD45RA^{high}CD69$^+$).[1,2,13] On the other hand, Depuydt et al[6] demonstrated that these CD69$^+$ effector memory T cells show signs of clonal expansion and recent TCR activation, arguing that T cells in the lesion can also express CD69 as a result of antigen recognition.

In this study, we aimed to assess the phenotype, proportion, and function of T_{RM} cells in the atherosclerotic lesion. To interrogate the phenotype of T cells in the lesion, we used single-cell RNA-sequencing (scRNA-seq) data of human atherosclerotic lesions and performed FACS analysis for T_{RM} cell–associated molecules on lymphocyte preparations isolated from mouse atherosclerotic lesions. To evaluate the proportion and function of T_{RM} cells in atherosclerotic lesions, a bone marrow transplantation study was performed, in which the formation of T_{RM} cells was hindered.

MATERIALS AND METHODS

The data that support the findings of this study are available from the corresponding author upon reasonable request.

Human Studies

Handling of all human samples complied with the Code for Proper Secondary Use of Human Tissue and is in accordance with the Declaration of Helsinki regarding ethical principles for medical research involving human subjects, and all patients signed an informed consent form. To evaluate the proportion of T_{RM} cell marker expressing T cells in the atherosclerotic lesion, atherosclerotic plaque samples were obtained from 20 patients who underwent carotid endarterectomy surgery at the Haaglanden Medical Center, Westeinde, The Hague, the Netherlands (study approval number: 17-046; protocol number: NL57482.098.17). Only atherosclerotic plaques from primary carotid endarterectomy surgeries were included in this study.

Human Atherosclerotic Plaque Cell Isolation

Human endarterectomy samples were digested into a single-cell suspension following a previously described protocol.[6] In brief, lesions were digested into a single-cell suspension by cutting the tissue into pieces of ≈1 mm^2, followed by digestion with 2.5 mg/mL collagenase IV (Thermo Fisher Scientific), 0.25 mg/mL DNAse I (Sigma), 2.5 mg/mL Human Albumin Fraction V (MP Biomedicals) in RPMI 1640 for 30 minutes at 37 °C. After digestion, plaque tissue was mashed over a 70-µm strainer to create a single-cell suspension and washed in RPMI

1640. Cells were cryostored in CryoStor cell cryopreservation medium (Sigma-Aldrich) at −80 °C until further use.

scRNA-seq on Human Plaques

A previously published scRNA-seq data set was used to interrogate the phenotype of T_{RM} cells in the atherosclerotic lesion.[6] In brief, scRNA-seq was performed on PBMCs and atherosclerotic lesions of 3 male patients who underwent carotid endarterectomy. PBMCs and single-cell plaque suspensions were stained with TotalSeq-C antibodies against CD3 and CD14. Plaque suspensions were additionally stained for CD45. scRNA-seq was performed on PBMCs and live $CD45^+$ plaque cells, using 10× Genomics 5′ Single Cell Immune Profiling technology. Next, $CD3^+$ T cells were selected from all immune cells and subclustered.

Integration of T_{RM} Cell Data Set

To compare the phenotype of plaque resident T cells with T cells previously identified as T_{RM} cells, T_{RM} cells were selected from a published scRNA-seq data set containing gene expression data of T cells from human intestinal transplants, and integrated with the plaque T cells, following the Seurat introduction to scRNA-seq integration vignette.[14] In brief, raw data (Gene Expression Omnibus: GSE162687) were processed using Seurat omitting cells with gene expression <200 and >2500 or >10% mitochondrial genes from the data set.

To decrease the dimensionality of the normalized data and execute cell clustering, a principal component analysis was conducted. The initial 10 principal component analysis components were utilized for identifying clusters at a resolution of 0.4, following authors' description.

After integration of the predefined T_{RM} cells into the atherosclerosis data set, the curated data set was clustered based on the top 15 principal component analysis components and a resolution of 0.7. Next, classical T_{RM} cells, with high expression of *CD69*, *ITGAE* (integrin alpha E), and *ZNF683* (zinc finger protein 683), were selected from the integrated T_{RM} cell data set for projection onto and integration into the atherosclerosis scRNA-seq data set. Other T cells from the integrated data set were removed from the curated data set. Clusters were visualized using UMAP and annotated based on differential gene expression between clusters, identified by a Wilcoxon rank-sum test (FindMarkers function Seurat).

T_{RM} Gene Signature

T_{RM} gene signature was based on the core signature of T_{RM} cells previously described by Kumar et al[15] and the canonical transcription factors involved in T_{RM} cell differentiation. The signature included CD69, CA10, ITGA1 (integrin alpha 1), ITGAE, IL (interleukin)-2, IL-10, CXCR6, CXCL13, KCNK5, RGS1, CRTAM, DUSP6, PDCD1, ZNF683, PRDM1, and RUNX3. The AddModuleScore function was used to calculate the average expression level of the genes included in the T_{RM} gene signature.

Animals

C57BL/6J, $RAG1^{-/-}$ (RAG1 deficient), and $LDLr^{-/-}$ (low-density lipoprotein receptor knockout) mice were purchased from The Jackson Laboratory (Sacramento, CA) and bred in-house. Animals were kept under standard laboratory conditions, and food and water were provided ad libitum. All animal work was performed in female mice, to prevent sex-driven variation in atherosclerosis development. All work was in compliance with the Dutch government guidelines and Directive 2010/63/EU of the European Parliament, and experiments were approved by the Ethics Committee for Animal Experiments and the Animal Welfare Body of Leiden University (project number: 106002017887; study number: 8873–178).

Donor Mice

During the bone marrow transplant experiments, we used wild-type mice (C57BL/6J mice), Hobit (Homolog of Blimp-1 [B lymphocyte–induced maturation protein 1] in T cells)^{tdTomato} mice (B6-Tg(Zfp683-tdTomato-P2A-Cre-P2A-DTR)[16]; bone marrow obtained from Sanquin Research), and Hobit$^{KO/CRE}$Blimp-1$^{flox/flox}$ mice (Hobit$^{CRE/tdTomato}$×Blimp-1$^{flox/flox}$; bone marrow obtained from Sanquin Research[17,18]) as donor mice. Hobit^{tdTomato} mice exhibit 1 functional *Zfp683* allele, allowing normal Hobit regulation, and 1 dysfunctional allele, in which *Zfp683* has been replaced for a cassette containing tdTomato, CRE recombinase, and DTR genes separated by P2A sequences enabling tracking and manipulation of Hobit-expressing cells.[16] Hobit$^{KO/CRE}$Blimp-1$^{flox/flox}$ mice have 2 disrupted *Zfp683* alleles.[17,18] One allele has been replaced with the tdTomato-P2A-Cre-P2A-DTR cassette, whereas the other allele has been disrupted with a gene-trapping construct. *Zfp683*-induced expression of Cre recombinase leads to the excision of the LoxP flanked exon 6 of the *Prdm1* gene, resulting in dysfunctional Blimp-1 in cells with an active *Zfp683* locus and, therefore, preventing the formation of T_{RM} cells. This *Zfp683*-Cre floxed *Prdm1* system knocks out Blimp-1 with 80% efficiency.

Bone Marrow Transplant

Forty-five female $RAG1^{-/-}LDLr^{-/-}$ mice of 8 to 16 weeks of age were exposed to 9 Gy (2×4.5 Gy, 0.19 Gy/min, 200 kV, 4 mA) total body irradiation using an Andrex Smart 225 Röntgen source (YXLON International) with a 6-mm aluminum filter to induce bone marrow aplasia. Mice received $10×10^6$ donor bone marrow cells originating from either wild-type mice (C57BL/6 mice), Hobit^{tdTomato} mice (Hobit$^{+/tdTomato}$ mice; bone marrow obtained from Sanquin laboratories), or Hobit$^{KO/CRE}$Blimp-1$^{flox/flox}$ mice (Hobit$^{CRE/tdTomato}$×Blimp$^{flox/flox}$; bone marrow obtained from Sanquin laboratories) in 100-µL saline via tail vein injection. Bone marrow was isolated by flushing the femoralis and tibia with PBS and passing the cells through a 70-µm cell strainer (Greiner Bio-One). During the recovery period of 4 weeks, the drinking water of the mice was supplemented with antibiotics (83 mg/L ciprofloxacin, 67 mg/L polymyxin B sulfate, and 6.5 g/L sucrose). After recovery, the mice were fed a Western-type diet (0.25% cholesterol and 15% cacao butter; Special Diet Services) for 10 weeks to induce lesion formation. Upon euthanization, the mice were anesthetized intraperitoneally with a mix of ketamine (100 mg/mL) and xylazine (10 mg/mL). Blood was collected via orbital bleeding, followed by perfusion with PBS through the left ventricle. The heart, aorta, spleen, and liver were collected for further analysis.

Organ Processing

Single-cell suspensions of the spleen and liver were obtained by using a 70-µm cell strainer (Greiner Bio-One). Red blood cells were removed from the liver, spleen, and blood samples by lysing the red blood cells for 2 minutes at room temperature with lysis buffer. To separate leukocytes from hepatocytes in the liver samples, gradient centrifugation with 35% Percoll (Merck) was applied. Aortas were cut into small fragments of ≈1 mm^2, and incubated with a digestion mix of collagenase I, 450 U/mL; collagenase XI, 250 U/mL; DNAse, 120 U/mL; and hyaluronidase, 120 U/mL (all Sigma-Aldrich) for 30 minutes at 37 °C while rotating. Digested aorta samples were passed over a 70-µm cell strainer to obtain a single-cell suspension. The upper part of the heart was embedded in Tissue-Tek OCT (Sakura) and stored at −80 °C until further usage.

Cholesterol Assay

Serum was obtained by collecting whole blood in cloth inducing microvette CB300Z tubes (Sarstedt), followed by centrifugation at 2000 RCF for 10 minutes at 4 °C. Serum was stored at −80 °C until further usage. Total cholesterol levels in serum were measured by performing an enzymatic colorimetric analysis (Roch/Hitachi, Germany), using Precipath standardized serum (1.69 mg/mL; Roche/Hitachi) as an internal standard.

Flow Cytometry

Around 500 000 cells, or all available cells, were stained with the appropriate antibodies (Table S1), Fc block (Biolegend), and live/dead viability staining (eBioscience) in PBS containing 2% FCS for 30 minutes at 4 °C. Before intracellular staining, the cells underwent fixation and permeabilization using an intracellular staining kit (eBioscience) or an intranuclear staining kit (FOXP3/transcription factor staining buffer set; eBioscience), following the manufacturer's instructions. To assess cytokine production, the cells were stimulated for 4 hours with phorbol 12-myristate 13-acetate (50 ng/mL; Sigma-Aldrich) and ionomycin (500 ng/mL; Sigma-Aldrich) in the presence of brefeldin A (5 µg/mL; ThermoScientific) in complete RPMI at 37 °C and 5% CO_2. Flow cytometry measurements were performed on Cytoflex S (Beckman Coulter). Data analysis was performed using the FlowJo v10.7 software (Treestar). Gating strategies are visualized in Figures S7 through S9. For the identification of T_{RM} cells in human atherosclerotic lesions, samples with <50 $CD4^+$ or $CD8^+$ T cells were excluded.

Histological Analysis

The trivalve area of the hearts was sectioned at 7-µm thickness using a Leica CM1950 cryostat. The size of atherosclerotic plaques and the percentage of stenosis were determined using oil red O staining (Sigma-Aldrich). To assess collagen content and necrotic core size in the atherosclerotic lesions, Masson trichrome staining (Sigma-Aldrich) was performed. To determine macrophage content in the lesions, sections were immunohistochemically stained with a primary antibody targeting a macrophage-specific antigen (MOMA-2, monoclonal rat IgG2b, diluted 1:1000), followed by secondary antibody staining with biotinylated rabbit anti-rat IgG (BA-4001, Vector, diluted 1:200). The reaction was visualized using the ImPACT NovaRED Peroxidase (HRP) substrate (Vector). All sections were digitized using a Panoramic 250 Flash III slide scanner (3DHISTECH; Hungary). Data analysis was performed using the ImageJ software.

Statistical Analysis

Data analysis was performed using Prism 9.0 (GraphPad Software, Inc, San Diego, CA). Data are expressed as mean±SD for all analyses. Outliers were identified by an ROUT or Grubbs outlier test. Shapiro-Wilk normality test was used to test data for normal distribution. Normally distributed data were analyzed using a 2-tailed unpaired Student *t* test when comparing 2 groups or a 2-way ANOVA with Bonferroni multiple comparisons test when comparing 2 groups with multiple conditions. Non-normally distributed data were analyzed using a Mann-Whitney *U* test. Statistical analysis was performed using GraphPad Prism. Probability values of $P \leq 0.05$ were considered to be significant.

To evaluate differential gene expression between T_{RM}-like T cells in the atherosclerotic lesion and other lesion-derived T cells, the FindMarkers function was used. Differential gene expression was computed using a nonparametric Wilcoxon rank-sum test, and Bonferroni-corrected *P* values were determined considering the overall gene count in the data set. Visualization of the differential gene expression was performed using a Volcano plot, facilitated by the EnhancedVolcano package.

RESULTS

Quantification of the Proportion of T_{RM} Cells in Human Atherosclerotic Lesions

T_{RM} cells have been identified at the site of former inflammation in a large variety of tissues. Here, we interrogated T cells from human atherosclerotic lesions on a single-cell level, to thoroughly evaluate the presence of T_{RM} cells in atherosclerosis. T_{RM} cells are notoriously heterogenic between tissues, making it challenging to identify T_{RM} cells in unexplored tissues by flow cytometry. Therefore, we used an in-house scRNA-seq data set encompassing information on the transcriptome of 3 human atherosclerotic plaque samples, obtained via endarterectomy of the carotid artery, along with patient-matched blood samples.[6] Subclustering of T cells residing in the atherosclerosis lesion resulted in 11 clusters, including 2 mixed T-cell clusters (clusters 0 and 7), 1 regulatory cluster (cluster 5), 2 memory T-cell clusters (clusters 1 and 6), 2 exhausted T-cell clusters (clusters 9 and 10), 1 γδ T-cell cluster (cluster 8), 2 cytotoxic lymphocyte clusters (clusters 3 and 4), and 1 $GZMK^+$ T_{RM} cell–like cluster (cluster 2; Figure 1A).

To identify T_{RM} cells within the atherosclerotic lesions, we analyzed the expression of the canonical T_{RM} cell marker *CD69*, as well as markers strongly associated with a T_{RM} cell phenotype, such as *CD49A* and *ITGAE* (encoding CD103), and transcription factors essential

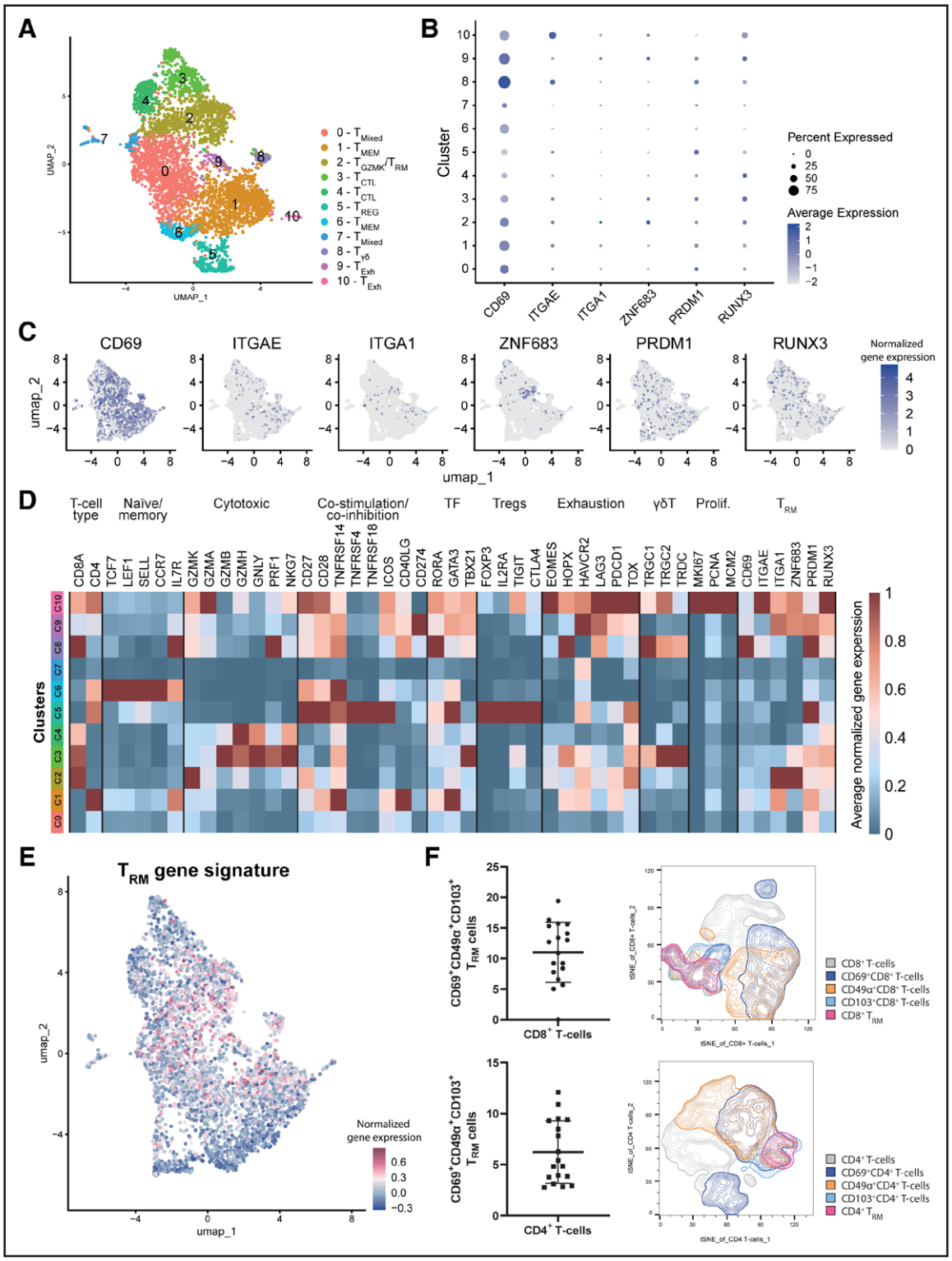

Figure 1. Resident memory T (T_{RM}) cell–associated marker expression in human atherosclerotic lesions.
A, UMAP representation of single-cell RNA-sequencing data of T cells from human atherosclerotic lesions (n=4548). **B**, Dot plot visualizing average T_{RM}-associated marker gene expression per cluster. **C**, Feature plot representation of T_{RM} marker expression. **D**, Heatmap displaying average expression of T-cell function–associated genes per cluster. **E**, Projection of T_{RM} gene signature onto UMAP representation of plaque-derived T cells. **F**, Flow cytometry analysis of CD69, CD49α, and CD103 expression by plaque-derived $CD4^+$ and $CD8^+$ T cells, demonstrating the percentage of $CD69^+CD49\alpha^+CD103^+$ coexpressing cells in a bar graph and tSNE representation. ITGA1 indicates integrin alpha 1; ITGAE, integrin alpha E; Prolif., proliferation; TF, tissue factor; Treg, T regulatory; and ZNF683, zinc finger protein 683.

for the formation of T_{RM} cells, including *ZNF683* (encoding HOBIT), *PRDM1* (encoding BLIMP-1), and *RUNX3*. T_{RM} cell–associated markers were mainly expressed by exhausted T-cell clusters 9 and 10 and by cytotoxic GZMK$^+$ cells from cluster 2 (Figure 1B through 1D). Projection of a T_{RM} gene signature, including core T_{RM} genes identified by Kumar et al and T_{RM} cell–associated transcription factors, onto the plaque-derived T cells identified clusters 0, 1, 2, 8, and 9 as clusters that potentially contain T_{RM} cells (Figure 1E). This T_{RM} gene signature was mainly expressed by T cells from the atherosclerotic lesion, and to a minor extent by T cells from circulation, confirming its specificity for tissue resident T cells (Figure S1). Moreover, coexpression of multiple T_{RM} cell markers, including CD69, CD49α, and CD103, was also confirmed on a protein level in human endarterectomy samples by flow cytometry (Figure 1F).

To more comprehensively evaluate how the phenotype of plaque-derived T cells relates to that of T_{RM} cells, T cells with a canonical T_{RM} cell phenotype (expressing CD69, ITGAE, and ZNF683) were selected from a previously published T_{RM} cell data set and integrated (Figure S2).[14] This T_{RM} cell data set consisted of scRNA-seq data of donor-derived T_{RM} cells extracted from intestinal transplant tissue 1 year after transplant using HLA (human leukocyte antigen) allele congenic cell tracking, ensuring the selection of long-lived T_{RM} cells. Reclustering of the curated data set resulted in 10 distinct T-cell clusters, with the predefined T_{RM} cells predominately coclustering with cells from cluster 3, demonstrating that a small proportion of plaque resident T cells exhibits a T_{RM}-like phenotype (≈4.6%; Figure 2A through 2C). The plaque-derived T cells from cluster 3 mainly originated from cluster 2 in the original clustering (Figure 2E), a cluster that was already associated with T_{RM} marker expression. To identify the expression profile of plaque-derived T cells from cluster 3, we excluded integrated T_{RM} cells from further analysis. T cells from cluster 3 were characterized by relatively high expression of T_{RM}-associated genes *CD69*, *ITGAE*, *ITGA1*, *ZNF683*, and *RUNX3* (Figure 2D). Moreover, genes associated with T-cell activation and cytotoxicity, including *KLRK1* (NKG2D), *CCL5*, *MATK*, *KLRC4*, and *CTSW* (encoding cathepsin C), were among the top differentially expressed genes (Figure 2E), underlining the high cytolytic potential of the T_{RM}-like T cells in the lesion.

Phenotyping T_{RM} Cells in the Atherosclerotic Environment

As the scRNA-seq analysis suggests the presence of a minor subset of T_{RM} in atherosclerotic lesions of patients, we next aimed to address their presence and role in the pathogenesis of atherosclerosis in mice. To corroborate the presence of T_{RM} in atherosclerotic lesions, a bone marrow transplant study was performed in RAG1$^{-/-}$LDLr$^{-/-}$ mice, receiving bone marrow of Hobit reporter mice (Hobit^{tdTomato}). In Hobit^{tdTomato} mice, the *Znf683* promotor of one allele was inserted with the *tdTomato* gene, encoding a red fluorescent protein.[19] After reconstitution of the bone marrow, mice were fed a Western-type diet for 10 weeks to induce atherosclerosis.

To address whether the Hobit reporter allowed detection of T_{RM} after bone marrow transplantation, we first examined T_{RM} in the liver, which naturally contains these cells. We observed that the percentage of tdTomato$^+$ T cells in the liver varied from 2.5% to 8% for CD4$^+$ T cells and between 7% and 26% for CD8$^+$ T cells, which is consistent with the previously reported numbers of T_{RM} in livers of naive mice (Figure 3A; Figure S3A and S3B).[20] TdTomato$^+$ CD4$^+$ and CD8$^+$ T cells from the liver almost uniformly expressed CD69, whereas tdTomato$^-$ T cells harbored a limited number of CD69-positive cells. Moreover, tdTomato$^+$ CD4$^+$ and CD8$^+$ T cells expressed significantly elevated levels of CD49α, compared with their tdTomato$^-$ counterparts. The increased expression of CD69 and CD49α suggests that tdTomato$^+$ T cells indeed positively identify as T_{RM} cells.

Next, we analyzed the number of T_{RM} cells in the aortic arch, a primary site of atherosclerotic lesion development. The proportion of tdTomato expressing T cells in the atherosclerotic lesion ranged from 0% to 6% for CD4$^+$ T cells and between 1% to 7% for CD8$^+$ T cells (Figure 3B; Figure S3C and S3D). The proportion of CD69$^+$ cells was significantly increased in the tdTomato$^+$ T cells compared with the tdTomato$^-$ T cells. However, CD69 was not exclusively expressed by tdTomato$^+$ T cells in the aorta, in line with previous reports suggesting that CD69 is upregulated in lesion-derived T cells as a response to antigen-specific interactions. Hence, CD69 cannot be considered as a standalone marker for identifying T_{RM} cells in the lesion.

Additional markers that were evaluated as potential T_{RM} markers in the lesion were CD49α and CD103. TdTomato$^+$ T cells in the lesion trended toward an upregulated expression of CD49α. Moreover, almost all CD49α$^+$ cells also coexpressed CD69 (Figure S3E and S3F). Integrin CD103, on the other hand, is a canonical T_{RM} marker for T_{RM} cells in epithelial and mucosal tissues and is differentially expressed by T_{RM} cells in the lesion. Hobit$^+$ CD4$^+$ T cells expressed elevated CD103 levels compared with their Hobit$^-$ counterparts. Although CD103 was highly expressed by CD8$^+$ T cells in the atherosclerotic lesion, it appeared to be mainly expressed by tdTomato$^-$ CD8$^+$ T cells as opposed to tdTomato$^+$ CD8$^+$ T cells, demonstrating CD103 alone is not a suitable marker for identifying CD8$^+$ T_{RM} cells in atherosclerosis. Coexpression of CD103 together with CD69, however, was almost exclusive to tdTomato$^+$ T cells, compared with tdTomato$^-$ cells (Figure S3E and S3F). Taken it all together, tracking of T_{RM} cells revealed CD69 and CD49α as markers characteristic for T_{RM} in the atherosclerotic lesion.

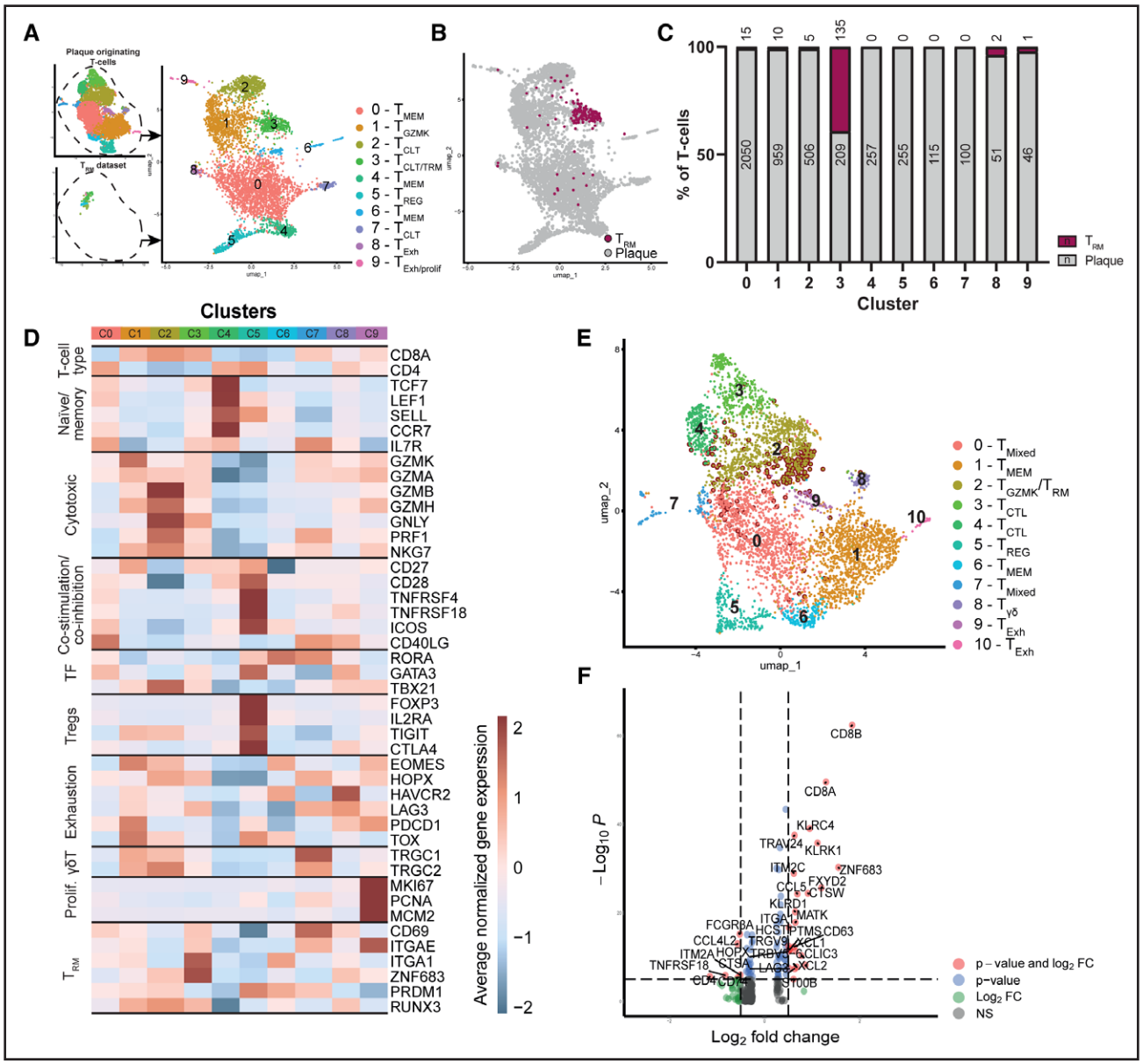

Figure 2. Predefined resident memory T (TRM) cells cluster together with plaque-derived T cells.
A, UMAP representation after integration of (**left**) plaque-derived T cells from the atherosclerosis single-cell RNA-sequencing (scRNA-seq) data set, and (**right**) predefined T_{RM} cells. **B**, Projection of predefined T_{RM} cells on unsupervised T-cell clustering of the curated data set. **C**, Percentage of integrated T_{RM} cells per cluster, with the number of integrated cells per cluster on top of each bar and the number of plaque-derived T cells in the middle of each bar. **D**, Heatmap displaying average expression of T-cell function–associated genes per cluster. **E**, UMAP representation of scRNA-seq data of T cells from human atherosclerotic lesions (clustering before integration), highlighting plaque-derived T cells from cluster 3 (clustering after integration). Highlighted cells are indicated with a read halo. **F**, Volcano plot displaying significantly differentially expressed genes of plaque-derived T cells from cluster 3, compared with T cells from all other clusters. Significantly differentially expressed genes were identified by the Wilcoxon rank-sum test, reaching statistical significance from $P<10^{-6}$. Prolif. indicates proliferation; TF, tissue factor; and Treg, T regulatory.

T_{RM} Cells Constitute Only a Minor Population in Atherosclerotic Lesions

Next, we set out to discover the role of T_{RM} cells in the pathogenesis of atherosclerosis. Blimp-1 and Hobit are central regulators of the conversion of T cells to a tissue resident phenotype in both classical and innate lymphocytes.[20] To investigate the function of T_{RM} in atherosclerosis, we performed a bone marrow transplant experiment with bone marrow originating from $Hobit^{KO/CRE}Blimp\text{-}1^{flox/flox}$ mice ($Hobit^{CRE/tdTomato}\times Blimp\text{-}1^{flox/flox}$ mice) or wild-type mice (C57BL/6 mice) transferred to $RAG1^{-/-}LDLr^{-/-}$ mice (Figure S4A). By knocking out Hobit and conditionally disrupting Blimp-1 in cells with an active *Znf683* promotor, the formation of T_{RM} cells can be severely reduced.[18,20]

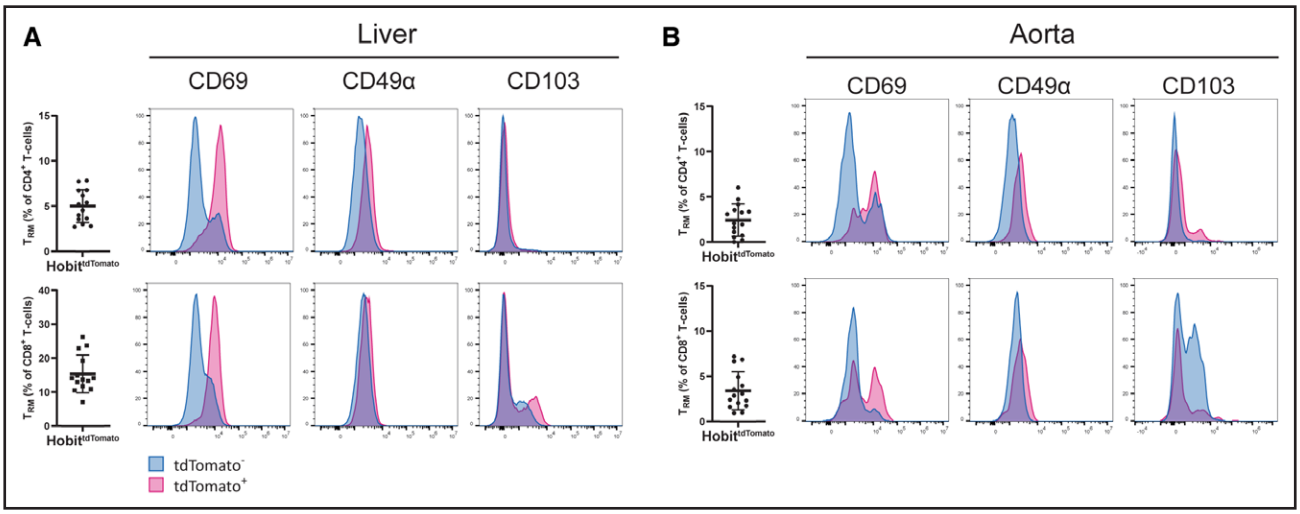

Figure 3. Lesion-derived resident memory T (T_{RM}) cells are characterized by elevated expression of CD69 and CD49α.
The percentage of Hobit (homolog of Blimp-1 [B lymphocyte–induced maturation protein 1] in T cells) expressing tdTomato⁺ CD4⁺ and CD8⁺ T cells and the expression of CD69, CD49α, and CD103 by tdTomato⁺ (pink) and tdTomato⁻ (blue) in the liver (**A**) and in the aorta (**B**).

Hobit$^{CRE/tdTomato}$×Blimp-1$^{flox/flox}$ mice exhibit a significantly reduced number of T_{RM}.[18] Moreover, the tdTomato⁺ T_{RM} progenitor cells that remained expressed reduced levels of retention molecule CD69, as well as increased levels of tissue egress markers S1PR1 and CCR7, demonstrating that these cells are not capable of obtaining a mature T_{RM} phenotype. After recovery of the bone marrow transplant, mice were fed a Western-type diet for 10 weeks to induce atherosclerosis formation. Throughout the experiment, mouse weights and cholesterol levels were similar between groups (Figure S4A through S4C). At the end of the experiment, the hampered formation of T_{RM} cells was confirmed in the liver by evaluating CD69⁺ T-cell counts (Figure S5).

The blocked T_{RM} formation resulted in some variations in circulating immune cell levels, while leukocyte populations in secondary lymphoid organs remained unaffected (Figure S4D and S4E). Given that Hobit and Blimp-1 are important for the differentiation of innate lymphoid cells as well, the distribution of natural killer (NK) cells and natural killer T (NKT) cells in the liver was evaluated.[20,21] The fraction of NK and NKT cells, which are low due to the bone marrow transplantation, were significantly reduced in the livers of Hobit$^{KO/CRE}$Blimp-1$^{flox/flox}$ mice (Figure S4F). Also, the cytolytic capacity of NK cells was affected by the Hobit/Blimp-1 knockout, apparent from a significantly reduced GZMB⁺ NK-cell population.

In the lesion, however, general leukocyte levels and T-cell numbers were not affected by the knockdown of T_{RM} cells (Figure 4A through 4E and 4G). Interestingly, we also did not observe changes in the CD69⁺ or CD49α⁺ T-cell populations and only a modest decrease in the percentage of CD69⁺CD49α⁺ double-positive CD8⁺ T cells (Figure 4F and 4H; Figure S6). The marginal changes in T_{RM} marker expressing T-cell populations underlines that T_{RM} cells only encompass a minor population in the atherosclerotic lesion.

T_{RM} Cells Associate With Reduced Macrophage Content and Increased Collagen Deposition in Atherosclerotic Lesions

To verify the effects of the Hobit/Blimp-1 conditional double knockout on the progression of atherosclerosis, plaque size and composition were assessed in the aortic root lesions of the heart by histological analysis. Neutral lipid staining of the lesions by oil red O demonstrated similar absolute plaque sizes, with a plaque size of ≈400 000 μm² and comparable vascular occlusion of ≈40% between groups (Figure 5A). Although plaque size was not altered by the lack of T_{RM} cells, plaque composition was affected in the Hobit$^{KO/CRE}$Blimp-1$^{flox/flox}$ group. The macrophage-positive stained area as a relative to plaque size was significantly increased in Hobit$^{KO/CRE}$Blimp-1$^{flox/flox}$ mice, with a 1.33-fold increase compared with the wild-type control (Figure 5B). Interestingly, the increased macrophage content did not translate to increased necrotic core sizes, evaluated by Masson trichrome staining (Figure 5C). Collagen content, on the other hand, trended toward a reduction in Hobit$^{KO/CRE}$Blimp-1$^{flox/flox}$ mice.

DISCUSSION

Tissue T_{RM} cells are a relatively newly discovered T-cell subset that forms the first line of defense against secondary infections. Despite the growing body of knowledge, the precise role of this specialized T-cell subset in chronic inflammatory diseases remains largely elusive.[22,23] This study contributes valuable insight on the

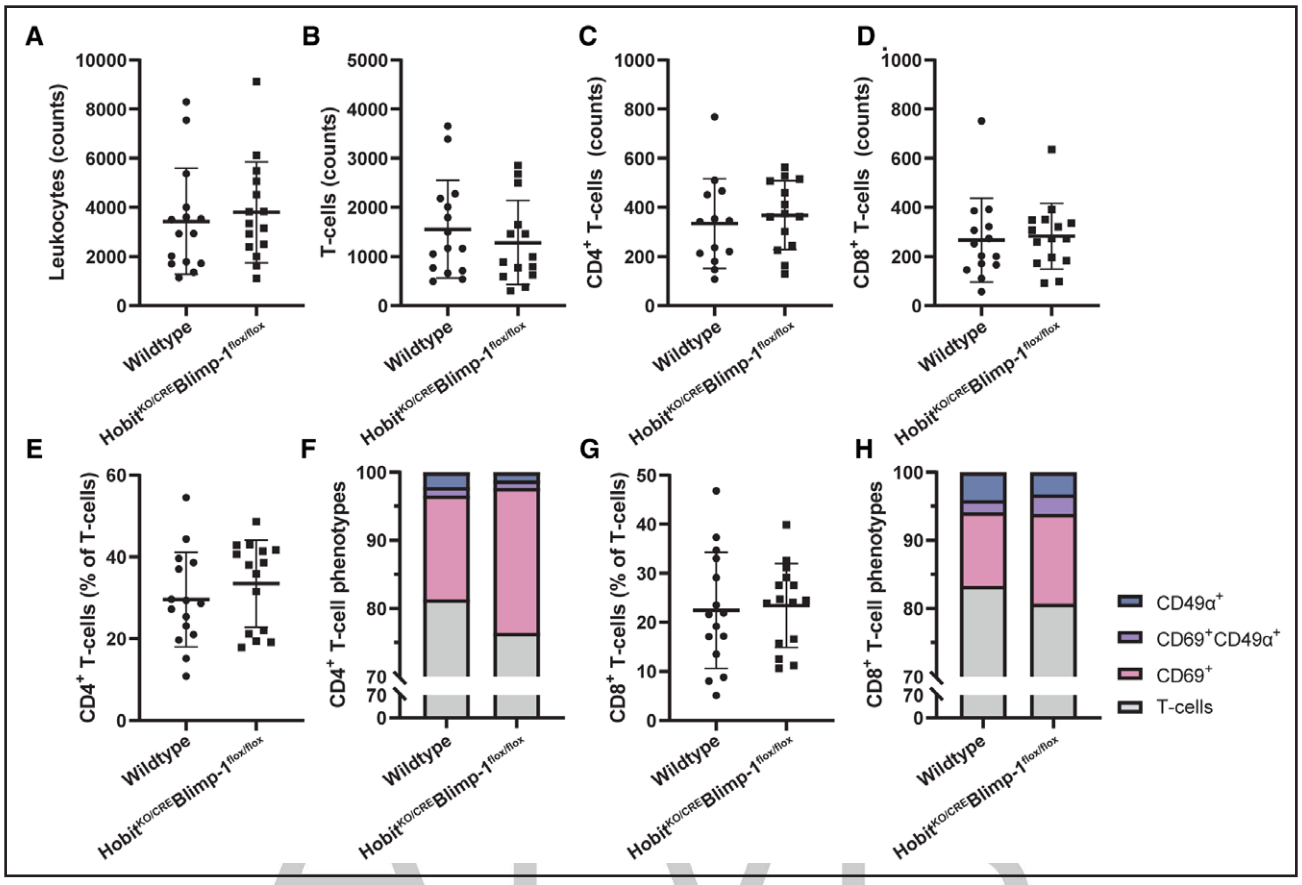

Figure 4. Reduction of resident memory T (T_{RM}) cells does not affect leukocyte numbers or T-cell populations in the atherosclerotic lesion.

Absolute leukocyte (CD45; **A**), T-cell (Thy1.2; **B**), $CD4^+$ T-cell ($Thy1.2^+CD4^+$; **C**), and $CD8^+$ T-cell ($Thy1.2^+CD8^+$; **D**) numbers in the aorta. **E**, Fraction of $CD4^+$ T cells (as a percentage of total T cells). **F**, Proportion of $CD69^+$, $CD49\alpha^+$, and $CD69^+CD49\alpha^+$ expressing $CD4^+$ T cells (as a percentage of total $CD4^+$ T cells). **G**, Fraction of $CD8^+$ T cells (as a percentage of total T cells). **H**, Proportion of $CD69^+$, $CD49\alpha^+$, and $CD69^+CD49\alpha^+$ expressing $CD8^+$ T cells (as a percentage of total $CD8^+$ T cells). Plots contain individual data points with mean±SD. Significance was determined by unpaired *t* test. Outliers were removed after an ROUT test. Blimp-1 indicates B lymphocyte–induced maturation protein 1; and Hobit, homolog of Blimp-1 in T cells.

presence, phenotype, and functionality of T_{RM} in both human and mouse atherosclerotic lesions. We demonstrated that T_{RM} cells constitute a minor fraction of the lymphocyte population in the atherosclerotic lesion and that mice in which the formation of T_{RM} was hindered exhibit increased lesion stability.

In human atherosclerotic lesions, we identified a minor population of T_{RM}-like cells that expressed elevated levels of T_{RM}-associated genes and coclustered with predefined T_{RM} cells for intestinal epithelium. Although the phenotype of these predefined T_{RM} cells might be affected by other microenvironmental circumstances (different tissue, disease, and medical background of the patient), they specifically clustered together with the plaque-derived T cells that expressed a T_{RM}-like phenotype in the unintegrated analysis, suggesting a common core T_{RM} signature for T_{RM} cells derived from different tissues.[15] The TRM-like cells in the atherosclerotic lesion were characterized by the expression of CD69, ITGA1, and ITGAE, on both transcriptional and translational levels, and a transcription factor profile associated with the T_{RM} phenotype.

The upregulated expression of CD69 and CD49α was corroborated in mice. Although human T_{RM} cells might be characterized by the expression of CD103, as shown here and by others[2]; this marker was inconsistently expressed by Hobit-expressing $CD4^+$ and $CD8^+$ T cells in mouse atherosclerotic lesions. Various studies demonstrated species-specific differences in the T_{RM} phenotype within the same tissue.[24] Moreover, T_{RM} cells located in nonepithelial/mucosal tissues often refrain from expressing CD103, as its ligand, E-cadherin, is not expressed there.[25] Controversially, a large proportion of $Hobit^-$ $CD8^+$ T cells did express CD103 in the atherosclerotic lesion. CD103 expression is enhanced by exposure to TGF-β (transforming growth factor beta), a cytokine expressed in atherosclerotic lesions and associated with protection against plaque rupture.[26,27]

Like the expression of CD103, the expression of CD69 was also not confined to T_{RM} cells. A substantial population

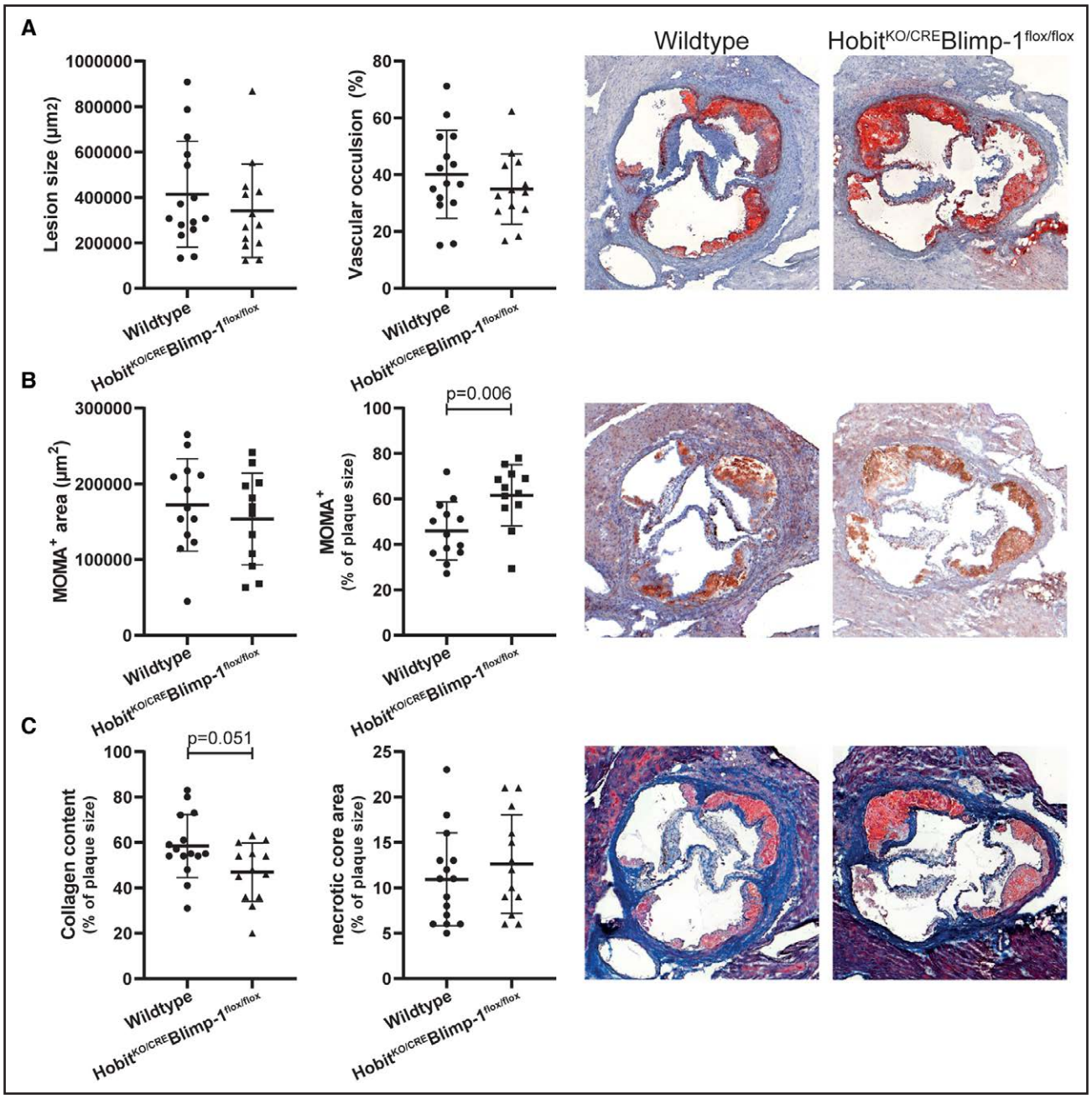

Figure 5. Hindered resident memory T (T_{RM}) cell formation results in a relative increase in intralesional macrophages and reduction in collagen content.

A, Quantification of lesion size and vascular occlusion in the trivalve area determined by oil red O staining and representative pictures of the wild-type and Hobit (homolog of Blimp-1 [B lymphocyte–induced maturation protein 1] in T cells)$^{KO/CRE}$Blimp-1$^{flox/flox}$ groups. **B**, Quantification of absolute and relative monocyte/macrophage content in the plaque by MOMA staining and representative pictures of the lesions. **C**, Quantification of relative necrotic core area and relative collagen content in the lesions after Masson trichrome staining and representative pictures of the lesions. Plots contain individual data points with mean±SD. Significance was determined by unpaired *t* test. Outliers were removed after an ROUT test.

of ≈20% of the CD4$^+$ and CD8$^+$ T cells expressed CD69 in mouse atherosclerotic lesions. However, on average, only 2.4% of the T cells expressed Hobit, suggesting that the majority of CD69-positive cells did not identify as T_{RM}. Lesional T cells have been reported to express an activated phenotype and display signs of clonal expansion and tissue enrichment, implying recent activation through TCR-specific interactions.[6,28] Hence, it seems that merely a fraction of CD69-expressing cells in the lesion possess a T_{RM} phenotype, while for the remaining cells potentially upregulated CD69 as a response to antigen recognition.

One limitation of our approach is that by identifying T_{RM} cells based on Hobit expression, we may have

underestimated the T_{RM} population. Although Hobit is exclusively expressed by T_{RM}, and not by other antigen-experienced T-cell populations, this marker might be downregulated over time by some T_{RM} cells, rendering identification in this study setup impossible.[16,18] Nonetheless, the knockdown of T_{RM} cells did not impact the proportion of T cells in the lesion nor the percentage of CD69 expressing T cells, indicating that T_{RM} population is indeed a small fraction of the T-cell population.

In spite of their modest representation, we did observe a significantly reduced plaque stability and increased macrophage content when T_{RM} cells were significantly reduced. However, these effects might not be fully attributable to the lack of T_{RM} cells, as we also observed changes in circulating leukocyte levels and a significant reduction in innate lymphocyte populations. Although NK and NKT cells have been detected inside atherosclerotic lesions, their function in atherosclerosis remains controversial. A recent study on the function of NK cells in atherosclerosis concluded that depletion of NK cells does not affect the progression of atherosclerosis.[29] In addition, most reports focusing on the function of NKT cells in atherosclerosis describe an aggravating effect of NKT cells in atherosclerosis, which does not explain the effects observed in this study.[30]

Moreover, similar protective effects were observed when all $CD8^+$ T cells, including all cytotoxic T cells, were depleted from advanced atherosclerotic lesions[31] or when $CD4^+$ T-cell numbers were strongly reduced and their interaction with MHCII was negated.[32] In line with previous reports focusing on the phenotype of T_{RM} cells, scRNA-seq of human atherosclerotic lesions revealed that T_{RM}-like cells in the lesion expressed high levels of granzymes and other cytotoxicity-associated molecules.[33] These cytolytic T cells might control intralesional macrophage content by specifically targeting macrophages. Moreover, antigen-specific CD8+ T cells have also been shown to exert atheroprotective effects.[34,35] The observed changes in collagen content might be a result of the relatively increased macrophage population, as macrophages express a variety of matrix degrading enzymes, like metalloproteinases, that contribute to the breakdown of the collagen in the fibrous cap.[36,37]

Interestingly, in most immune disorders, like rheumatoid arthritis, inflammatory bowel disease, and psoriasis, T_{RM} cells are associated with disease acceleration. Yet, unlike atherosclerosis, these diseases are characterized by a relapsing-remitting course, and T_{RM} cells have been implicated to contribute to these reoccurring disease flares.[10,11,38] Atherosclerosis, on the other hand, is an ongoing chronic inflammatory disease characterized by constant immune cell infiltration, persistent chemokine and cytokine production, and continuous antigen presentation.[6] The chronic nature of the disease might explain the limited formation of T_{RM} cells in the lesion. Although some reports argue persistent low-gradient antigen presentation induces memory inflation and increases T_{RM} populations,[39] others showed compromised T_{RM} formation after chronic viral infection, compared with acute infection.[40]

In conclusion, this study provides valuable insights into the presence, phenotype, and function of tissue-T_{RM} cells in human and mouse atherosclerotic lesions. We demonstrate that intralesional T_{RM} cells are characterized by the expression of CD69 and CD49α and that although these T_{RM} cells only constitute a minor T-cell population within the lesion, their presence was associated with reduced atherosclerotic burden by decreasing the amount of intralesional macrophages and enhancing lesion stability.

ARTICLE INFORMATION

Received November 29, 2023; accepted March 14, 2024.

Affiliations

Division of Biotherapeutics, Leiden Academic Centre for Drug Research, Leiden University, the Netherlands (M.J.M.d.J., M.A.C.D., F.H.S., K.L., D.M., J.K., I.B., B.S.). van Gisbergen Lab, Tissue Immunity, Champalimaud Research, Lisbon, Portugal (K.v.G.). Department of Surgery, Haaglanden Medical Center, The Hague, the Netherlands (A.W., H.J.S.).

Sources of Funding

This work was supported by the Dutch Heart Foundation (CVON2017-20: GENIUS II, awarded to J. Kuiper), European Research Area Network on Cardiovascular Diseases (ERA-CVD, 2018T092, awarded to B. Slütter).

Disclosures

None.

Supplemental Material

Figures S1–S10
Table S1
Major Resources Table

REFERENCES

1. Depuydt MAC, Prange KHM, Slenders L, Örd T, Elbersen D, Boltjes A, De Jager SCA, Asselbergs FW, De Borst GJ, Aavik E, et al. Microanatomy of the human atherosclerotic plaque by single-cell transcriptomics. *Circ Res.* 2020;127:1437–1455. doi: 10.1161/CIRCRESAHA.120.316770
2. Fernandez DM, Rahman AH, Fernandez NF, Chudnovskiy A, Amir E ad D, Amadori L, Khan NS, Wong CK, Shamailova R, Hill CA, et al. Single-cell immune landscape of human atherosclerotic plaques. *Nat Med.* 2019;25:1576–1588. doi: 10.1038/s41591-019-0590-4
3. Winkels H, Ehinger E, Vassallo M, Buscher K, Dinh HQ, Kobiyama K, Hamers AAJ, Cochain C, Vafadarnejad E, Saliba AE, et al. Atlas of the immune cell repertoire in mouse atherosclerosis defined by single-cell RNA-sequencing and mass cytometry. *Circ Res.* 2018;122:1675. doi: 10.1161/CIRCRESAHA.117.312513
4. Smit V, de Mol J, Schaftenaar F, Depuydt M, Postel R, Smeets D, Verheijen F, Bogers L, van Duijn J, Verwilligen R, et al. Single-cell profiling reveals age-associated immunity in atherosclerosis. *Cardiovasc Res.* 2023;119:2508. doi: 10.1093/cvr/cvad099
5. Saigusa R, Winkels H, Ley K. T cell subsets and functions in atherosclerosis. *Nat Rev Cardiol.* 2020;17:387–401. doi: 10.1038/s41569-020-0352-5
6. Depuydt MAC, Schaftenaar FH, Prange KHM, Boltjes A, Hemme E, Delfos L, De Mol J, De Jong MJM, Kleijn MNAB, Peeters JAHM, et al. Single-cell T cell receptor sequencing of paired human atherosclerotic plaques and blood reveals autoimmune-like features of expanded effector T cells. doi: 10.1038/s44161-022-00208-4
7. Urban SL, Berg LJ, Welsh RM. Type 1 interferon licenses naïve CD8 T cells to mediate anti-viral cytotoxicity. *Virology.* 2016;493:52–59. doi: 10.1016/j.virol.2016.03.005

8. Cibrián D, Sánchez-Madrid F. CD69: from activation marker to metabolic gatekeeper. *Eur J Immunol.* 2017;47:946–953. doi: 10.1002/eji.201646837
9. Zhang Z, Qiu S, Zhang X, Chen W. Optimized DNA electroporation for primary human T cell engineering. *BMC Biotechnol.* 2018;18:4. doi: 10.1186/s12896-018-0419-0
10. Zundler S, Becker E, Spocinska M, Slawik M, Parga-Vidal L, Stark R, Wiendl M, Atreya R, Rath T, Leppkes M, et al. Hobit- and Blimp-1-driven CD4+ tissue-resident memory T cells control chronic intestinal inflammation. *Nat Immunol.* 2019;20:288–300. doi: 10.1038/s41590-018-0298-5
11. Chang MH, Levescot A, Nelson-Maney N, Blaustein RB, Winden KD, Morris A, Wactor A, Balu S, Grieshaber-Bouyer R, Wei K, et al. Arthritis flares mediated by tissue-resident memory T cells in the joint. *Cell Rep.* 2021;37:109902. doi: 10.1016/j.celrep.2021.109902
12. Wang Z, Zhang X, Lu S, Zhang C, Ma Z, Su R, Li Y, Sun T, Li Y, Hong M, et al. Pairing of single-cell RNA analysis and T cell antigen receptor profiling indicates breakdown of T cell tolerance checkpoints in atherosclerosis. *Nat Cardiovasc Res.* 2023;2:290–306. doi: 10.1038/s44161-023-00218-w
13. Winkels H, Wolf D. Heterogeneity of T cells in atherosclerosis defined by single-cell RNA-sequencing and cytometry by time of flight. *Arterioscler Thromb Vasc Biol.* 2021;41:549–563. doi: 10.1161/ATVBAHA.120.312137
14. FitzPatrick MEB, Provine NM, Garner LC, Powell K, Amini A, Irwin SL, Ferry H, Ambrose T, Friend P, Vrakas G, et al. Human intestinal tissue-resident memory T cells comprise transcriptionally and functionally distinct subsets. *Cell Rep.* 2021;34:108661. doi: 10.1016/j.celrep.2020.108661
15. Kumar BV, Ma W, Miron M, Granot T, Guyer RS, Carpenter DJ, Senda T, Sun X, Ho SH, Lerner H, et al. Human tissue-resident memory T cells are defined by core transcriptional and functional signatures in lymphoid and mucosal sites. *Cell Rep.* 2017;20:2921–2934. doi: 10.1016/j.celrep.2017.08.078
16. Behr FM, Parga-Vidal L, Kragten NAM, van Dam TJP, Wesselink TH, Sheridan BS, Arens R, van Lier RAW, Stark R, van Gisbergen KPJM. Tissue-resident memory CD8+ T cells shape local and systemic secondary T cell responses. *Nat Immunol.* 2020;21:1070–1081. doi: 10.1038/s41590-020-0723-4
17. Van Gisbergen KPJM, Kragten NAM, Hertoghs KML, Wensveen FM, Jonjic S, Hamann J, Nolte MA, Van Lier RAW. Mouse Hobit is a homolog of the transcriptional repressor Blimp-1 that regulates NKT cell effector differentiation. *Nat Immunol.* 2012;13:864–871. doi: 10.1038/ni.2393
18. Parga-Vidal L, Taggenbrock RLRE, Beumer-Chuwonpad A, Aglmous H, Kragten NAM, Behr FM, Bovens AA, van Lier RAW, Stark R, van Gisbergen KPJM. Hobit and Blimp-1 regulate TRM abundance after LCMV infection by suppressing tissue exit pathways of TRMprecursors. *Eur J Immunol.* 2022;52:1095. doi: 10.1002/eji.202149665
19. Shaner NC, Campbell RE, Steinbach PA, Giepmans BNG, Palmer AE, Tsien RY. Improved monomeric red, orange and yellow fluorescent proteins derived from Discosoma sp. red fluorescent protein. *Nat Biotechnol.* 2004;22:1567–1572. doi: 10.1038/nbt1037
20. Mackay LK, Minnich M, Kragten NAM, Liao Y, Nota B, Seillet C, Zaid A, Man K, Preston S, Freestone D, et al. Hobit and Blimp1 instruct a universal transcriptional program of tissue residency in lymphocytes. *Science.* 2016;352:459–463. doi: 10.1126/science.aad2035
21. Kragten NA, Taggenbrock RL, Parga Vidal L, van Lier RA, Stark R, van Gisbergen KP. Hobit and Blimp-1 instruct the differentiation of iNKT cells into resident-phenotype lymphocytes after lineage commitment. *Eur J Immunol.* 2022;52:389. doi: 10.1002/eji.202149360
22. Wu H, Liao W, Li Q, Long H, Yin H, Zhao M, Chan V, Lau CS, Lu Q. Pathogenic role of tissue-resident memory T cells in autoimmune diseases. *Autoimmun Rev.* 2018;17:906. doi: 10.1016/j.autrev.2018.03.014
23. Samat AAK, van der Geest J, Vastert SJ, van Loosdregt J, van Wijk F. Tissue–resident memory T cells in chronic inflammation—local cells with systemic effects? *Cells.* 2021;10:1–19. doi: 10.3390/cells10020409
24. Szabo PA, Miron M, Farber DL. Location, location, location: tissue resident memory T cells in mice and humans. *Sci Immunol.* 2019;4:9673. doi: 10.1126/sciimmunol.aas9673
25. Behr FM, Chuwonpad A, Stark R, van Gisbergen KPJM. Armed and ready: transcriptional regulation of tissue-resident memory CD8 T cells. *Front Immunol.* 2018;9:1770. doi: 10.3389/fimmu.2018.01770
26. Edsfeldt A, Singh P, Matthes F, Tengryd C, Cavalera M, Bengtsson E, Dunér P, Volkov P, Karadimou G, Gisterå A, et al. Transforming growth factor-β2 is associated with atherosclerotic plaque stability and lower risk for cardiovascular events. *Cardiovasc Res.* 2023;119:2061–2073. doi: 10.1093/cvr/cvad079
27. El-Asady R, Yuan R, Liu K, Wang D, Gress RE, Lucas PJ, Drachenberg CB, Hadley GA. TGF-β–dependent CD103 expression by CD8+ T cells promotes selective destruction of the host intestinal epithelium during graft-versus-host disease. *J. Exp. Med.* 2005;201:1647. doi: 10.1084/jem.20041044
28. Chowdhury RR, D'Addabbo J, Huang X, Veizades S, Sasagawa K, Louis DM, Cheng P, Sokol J, Jensen A, Tso A, et al. Human coronary plaque T cells are clonal and cross-react to virus and self. *Circ Res.* 2022;130:1510–1530. doi: 10.1161/CIRCRESAHA.121.320090
29. Behr FM, Parga-Vidal L, Kragten NAM, van Dam TJP, Wesselink TH, Sheridan BS, Arens R, van Lier RAW, Stark R, van Gisbergen KPJM. Tissue-resident memory CD8+ T cells shape local and systemic secondary T cell responses. *Nat Immunol.* 2020;21:1070–1081. doi: 10.1038/s41590-020-0723-4
30. Nour-Eldine W, Joffre J, Zibara K, Esposito B, Giraud A, Zeboudj L, Vilar J, Terada M, Bruneval P, Vivier E, et al. Genetic depletion or hyperresponsiveness of natural killer cells do not affect atherosclerosis development. *Circ Res.* 2018;122:47–57. doi: 10.1161/CIRCRESAHA.117.311743
31. Chakrabarti R, Duddu S, Tiwari A, Naidu KT, Sharma P, Chakravorty N, Shukla PC. Natural killer T cells and the invariant subset promote atherosclerosis: a meta-analysis. *Life Sci.* 2023;321:121620. doi: 10.1016/j.lfs.2023.121620
32. Van Duijn J, Kritikou E, Benne N, Van Der Heijden T, Van Puijvelde GH, Kröner MJ, Schaftenaar FH, Foks AC, Wezel A, Smeets H, et al. CD8+ T-cells contribute to lesion stabilization in advanced atherosclerosis by limiting macrophage content and CD4+ T-cell responses. *Cardiovasc Res.* 2019;115:729–738. doi: 10.1093/cvr/cvy261
33. Wigren M, Rattik S, Yao Mattisson I, Tomas L, Grönberg C, Söderberg I, Alm R, Sundius L, Ljungcrantz I, Björkbacka H, et al. Lack of ability to present antigens on major histocompatibility complex class II molecules aggravates atherosclerosis in ApoE-/- mice. *Circulation.* 2019;139:2554–2566. doi: 10.1161/CIRCULATIONAHA.118.039288
34. Cheuk S, Schlums H, Gallais Sérézal I, Martini E, Chiang SC, Marquardt N, Gibbs A, Detlofsson E, Introini A, Forkel M, et al. CD49a expression defines tissue-resident CD8+ T cells poised for cytotoxic function in human skin. *Immunity.* 2017;46:287. doi: 10.1016/j.immuni.2017.01.009
35. Chyu KY, Zhao X, Dimayuga PC, Zhou J, Li X, Yano J, Lio WM, Chan LF, Kirzner J, Trinidad P, et al. CD8 + T cells mediate the athero-protective effect of immunization with an ApoB-100 peptide. *PLoS One.* 2012;7:e30780. doi: 10.1371/journal.pone.0030780
36. Dimayuga PC, Zhao X, Yano J, Lio WM, Zhou J, Mihailovic PM, Cercek B, Shah PK, Chyu KY. Identification of apoB-100 peptide-specific CD8+ T cells in atherosclerosis. *J Am Heart Assoc.* 2017;6:e005318. doi: 10.1161/JAHA.116.005318
37. Libby P, Geng YJ, Aikawa M, Schoenbeck U, Mach F, Clinton SK, Sukhova GK, Lee RT. Macrophages and atherosclerotic plaque stability. *Curr Opin Lipidol.* 1996;7:330–335. doi: 10.1097/00041433-199610000-00012
38. Newby AC. Metalloproteinase production from macrophages - a perfect storm leading to atherosclerotic plaque rupture and myocardial infarction. *Exp Physiol.* 2016;101:1327–1337. doi: 10.1113/EP085567
39. Chen L, Shen Z. Tissue-resident memory T cells and their biological characteristics in the recurrence of inflammatory skin disorders. *Cell Mol Immunol.* 2020;17:64. doi: 10.1038/s41423-019-0291-4
40. Uddbäck I, Cartwright EK, Schøller AS, Wein AN, Hayward SL, Lobby J, Takamura S, Thomsen AR, Kohlmeier JE, Christensen JP. Long-term maintenance of lung resident memory T cells is mediated by persistent antigen. *Mucosal Immunol.* 2021;14:92. doi: 10.1038/s41385-020-0309-3
41. Casey KA, Fraser KA, Schenkel JM, Moran A, Abt MC, Beura LK, Lucas PJ, Artis D, Wherry EJ, Hogquist K, et al. Antigen-independent differentiation and maintenance of effector-like resident memory T cells in tissues. *J Immunol.* 2012;188:4866–4875. doi: 10.4049/jimmunol.1200402